Biophysical Mechanisms of Transient Optical Stimulation of Peripheral Nerve

Jonathon Wells,* Chris Kao,* Peter Konrad,* Tom Milner,† Jihoon Kim,† Anita Mahadevan-Jansen,* and E. Duco Jansen*

*Department of Biomedical Engineering and Department of Neurosurgery, Vanderbilt University, Nashville, Tennessee 37235; and †Department of Biomedical Engineering, University of Texas at Austin, Austin, Texas

ABSTRACT A new method for in vivo neural activation using low-intensity, pulsed infrared light exhibits advantages over standard electrical means by providing contact-free, spatially selective, artifact-free stimulation. Here we investigate the biophysical mechanism underlying this phenomenon by careful examination of possible photobiological effects after absorption-driven light-tissue interaction. The rat sciatic nerve preparation was stimulated in vivo with a Holmium:yttrium aluminum garnet laser (2.12 μm), free electron laser (2.1 μm), alexandrite laser (750 nm), and prototype solid-state laser nerve stimulator (1.87 μm). We systematically determined relative contributions from a list of plausible interaction types resulting in optical stimulation, including thermal, pressure, electric field, and photochemical effects. Collectively, the results support our hypothesis that direct neural activation with pulsed laser light is induced by a thermal transient. We then present data that characterize and quantify the spatial and temporal nature of this required temperature rise, including a measured surface temperature change required for stimulation of the peripheral nerve (6°C–10°C). This interaction is a photothermal effect from moderate, transient tissue heating, a temporally and spatially mediated temperature gradient at the axon level (3.8°C–6.4°C), resulting in direct or indirect activation of transmembrane ion channels causing action potential generation.

INTRODUCTION

The basis of this work is to reveal the mechanism by which pulsed laser light can be used for contact-free, damage-free, artifact-free stimulation of discrete populations of neural fibers. We have previously shown that a pulsed, low-energy laser beam elicits compound nerve and muscle action potentials, with resultant muscle contraction, which is indistinguishable from responses obtained with conventional bipolar electrical stimulation of the rat sciatic nerve in vivo (1,2). The stimulation threshold (0.3–0.4 J/cm^2) at optimal wavelengths in the infrared (2.1, 1.87 μm) is ~2.5 times less than the threshold at which histological tissue damage occurs (0.8–1.0 J/cm^2). Although our studies have shown that optical stimulation is an effective and advantageous method for stimulation, the obvious question of the underlying mechanism is largely unanswered. Before we can understand the biological mechanism responsible for transient optical nerve stimulation, it is critical to consider the effects in neural tissue upon light interaction. Realization of these biophysical processes will ultimately help to refine an optimal laser parameter set to effectively target the diverse morphology of neural tissue types as well as identify possible clinical applications and limitations for this nerve stimulation modality.

Initially, it is important to build a conceptual understanding of the laser-tissue interactions that occur during optical nerve stimulation. The use of lasers in medical procedures can be grouped into two distinct categories: therapeutic and diagnostic or imaging applications. Regardless of the application, the interaction between the laser and biological tissue results in light distribution and absorption leading to subsequent photobiological effects. These effects can be separated into three potentially mechanistic categories: 1) photochemical, 2) photothermal, and 3) photomechanical (for review see Jacques (3)). The duration of the laser exposure, which is largely similar to the interaction time itself, together with the wavelength distinguish and primarily control these photobiological processes. It is worth noting here that others have previously demonstrated action potential generation in neurons through chemical, thermal, and mechanical means (4–6). Photochemical effects depend on the absorption of light to act as a reagent in a stoichiometric reaction catalyzed by a specific photosensitizer. An example of a photochemical effect is the production of reactive chemicals (ultimately leading to oxygen radicals) reported in photodynamic therapy by the combination of an injected extrinsic dye and light (7–9). Frequently, low-level light therapy is also attributed to photochemical interactions thought to target natural intrinsic agents, although this is not scientifically ascertained (10,11). Photothermal effects result from the transformation of absorbed light energy to heat, which may lead to hyperthermia, coagulation, or ablation of the target tissue (12). Photomechanical effects are secondary to rapid heating with short laser pulses (<1 μs) that produce mechanical forces, such as explosive events and laser-induced pressure waves able to disturb cells and tissue (13,14). The latter can be further separated into three distinct categories, including thermoelastic

Submitted January 18, 2007, and accepted for publication May 22, 2007.

Address reprint requests to E. Duco Jansen, PhD, Associate Professor in Biomedical Engineering and Neurological Surgery, 5805 Stevenson Center, Vanderbilt University, 2201 West End Avenue, Nashville, TN 37235. Tel.: 615-343-1911; Fax: 615-343-7919; E-mail: duco.jansen@vanderbilt.edu.

Editor: Francisco Bezanilla.

0006-3495/07/10/2567/14 $2.00

doi: 10.1529/biophysj.107.104786

expansion, ablative recoil, and expansion secondary to temperature increase or phase change (15).

In a majority of therapeutic laser applications, laser-tissue interaction is mediated by a thermal or thermomechanical process depending on the operational parameters of the laser, such as wavelength (λ), pulse duration (τ), and laser radiant exposure or irradiance. Typically, laser radiant exposure (J/cm^2) associated with most therapeutic procedures results in either reversible or nonreversible thermal or mechanical alterations of the tissue. The key parameter, wavelength, determines light distribution in the tissue dictated by wavelength-dependent optical properties. The energy density and subsequent temperature rise resulting from absorption of optical energy is inversely proportional to the penetration depth and, depending on the laser radiant exposure, a temperature increase is induced in the tissue (for comprehensive review see Thomsen (16)). In general, the objective is to damage tissue locally by exploiting high spatial precision and the ability to couple laser light into fiber optics for minimally invasive delivery to the tissue (17). Although optical nerve stimulation does exploit these distinctive delivery advantages, the result of this technique is a stimulation effect in tissue rather than destruction. Although photochemical processes are often governed by a specific reaction pathway, photothermal effects are nonspecific and are mediated by absorption of optical energy and governed by fundamental principles of heat transport. Subsequent effects in the target tissue are determined by the temperature rise and the duration of the temperature exposure as described by an Arrhenius rate process (18).

The hypothesis for this research asserts the biophysical mechanism responsible for pulsed laser stimulation of the nerve tissue is thermally mediated (thermal or thermomechanical processes) leading to direct activation of action potentials. This hypothesis is based on previous work demonstrating that the stimulation threshold varies as a function of tissue absorption (2). The null hypothesis postulation forms the experimental strategy to evaluate the contributions from other possible photobiological laser tissue interactions, such as photochemical, electric field, and photomechanical effects. The purpose of this article is to provide the scientific community with a conceptual understanding of the underlying mechanisms by which pulsed laser light allows selective excitation of neural tissue through both theoretical calculations and experimental evidence gathered from animal models in vivo. Studies are designed to systematically consider the four plausible physical mechanisms of action, including light electric field, photochemical, photomechanical, and photothermal tissue effects. Thermal effects in tissue are quantified in vivo with the use of an infrared camera. Understanding the biophysical processes may be expected to elucidate appropriate scientific routes to unravel the underlying physiological mechanisms at the membrane level. Ultimately, answers ascertained in this work will help refine optimal laser parameters for safe and effective stimulation of nerves and more importantly will define the uses most appropriate for clinical implementation.

MATERIALS AND METHODS

All animal experiments were conducted at the Vanderbilt University W. M. Keck Free Electron Laser Center and Vanderbilt Biomedical Optics Laboratory in accordance with standards set by the Institutional Animal Care and Use Committee.

Animal preparation

A total of 60 Spraque-Dawley rats (M/F 300–400 g) were used for the majority of these acute experiments. Four northern leopard frogs (2–3 inches) were pithed for a small subset of experiments. In preparation for surgery, each animal was anesthetized with intraperitoneal injection of ketamine (80 mg/kg) and xylazine (10 mg/kg) solution and maintained under sedative with additional boluses of ketamine for the duration of each individual experiment. Once anesthetized, the animal was placed in the prone position and the right and left sciatic nerve exposed over the length of the femur. An incision was made posterior-laterally extending from the gluteus muscles to the popliteal region. This allowed access to the sciatic nerve from its exit from the pelvic cavity to the level of the knee and allowed for visualization of specific motor branches (*n. fibularis* and *n. tibialis*) to the biceps femoris, gastrocnemius, and distal muscles. The muscle fascia overlying the nerve was carefully removed to expose the nerve surface with its epineurial (outer) covering maintained intact. Nerves were continually moistened with normal saline to avoid desiccation during the study.

Experimental design and electrophysiological evaluation

A bipolar recording electrode (Grass E-2 electrodes; Grass Telefactor, West Warwick, RI) was placed in contact with a site along the sciatic nerve distal to the site of stimulation to collect compound nerve action potentials (CNAPs) from motor axons. Compound muscle action potential (CMAP) recordings were made by placing needle electrodes into the innervated muscle in a bipolar fashion. Responses were recorded with a modular data acquisition system (MP100, Biopac Systems, Santa Barbara, CA) controlled using a laptop computer and Acknowledge software (Biopac Systems). For the purposes of this study, stimulation threshold was defined as the minimum radiant exposure incident on the peripheral nerve surface required for one visible muscle twitch per laser pulse. Recorded responses served to confirm the evoked stimulation and nerve potential propagation.

Laser setup

Four different lasers were used in these experiments, including the Holmium:yttrium aluminum garnet (Ho:YAG) laser (1-2-3 laser, Schwartz Electro Optics) operating at 2.12 μm with a pulse width of 350 μs (full width at half-maximum (FWHM)), alexandrite laser (1-2-3 laser, Schwartz Electro Optics, Orlando, FL) operating at 750 nm with a 350 μs pulse width, portable pulsed diode optical nerve stimulator (Aculight, Bothell, WA) operating at 1.87 μm with a tunable pulse width (1–10 ms), and the Free Electron Laser (FEL) at Vanderbilt University with a tunable wavelength from 2 to 10 μm and a 5-μs macropulse structure. We have provided evidence that pulsed laser light at $\lambda = 2.12$ μm is optimal for stimulation in the rat peripheral nerve (1); thus most experiments were performed using the Ho:YAG laser. This laser beam was coupled directly to a 600 μm optical fiber (3M Optical Fiber Power Core, FT-600-DMT; 3M, St. Paul, MN) mounted on a three-dimensional micromanipulator and precisely positioned over the nerve. The intensity of radiant exposure (0.3–1.0 J/cm^2) was controlled via attenuating optical filters.

Reported radiant exposures were calculated based on the spot size at the tissue, given the optical fiber diameter, the distance from fiber to tissue, and the numerical aperture of the fiber. In pulse duration studies the FEL was tuned to 2.1 μm and delivered as a free beam using a focusing lens with a spot size at the target tissue similar to the output from the Ho:YAG. The pulsed diode laser was also used in pulse duration studies. This solid-state laser diode, developed for these specific optical stimulation experiments emits at 1870 nm. This wavelength has an absorption coefficient in soft biological tissue similar to that of the Ho:YAG laser. As in the Ho:YAG laser experiments a 600 μm fiber was used to deliver equivalent radiant exposures using the Pulsed diode laser. Finally, a study to examine the effect of a laser-induced electric field on nerve stimulation utilized the Schwartz Electro Optics 1-2-3 configuration to create an alexandrite laser. This laser wavelength is different from that of the Ho:YAG and yields an absorption coefficient that is several orders of magnitude less; however, all other laser parameters as well as the setup for delivery remained unchanged.

OCT measurements

Surface displacement attributable to heat-induced volumetric expansion upon laser irradiation were measured using differential phase optical coherence tomography (DP-OCT) at the University of Texas in Austin (UTA) as described in Telenkov et al. (19), Rylander et al. (20), and Kim et al. (21). This system was employed to make use of its extremely high spatial (20 nm) and temporal (1 MHz) resolution measurement capabilities. Rat sciatic nerve tissue was extracted and immediately placed in a dish hydrated with saline and covered with a thin microscope slide coverslip for ex vivo experiments. The Ho:YAG laser coupled to a 600 μm fiber located 0.75 mm from the tissue was used to irradiate the tissue over a range of radiant exposures (0.3–1.0 J/cm^2). Differences in fringe signals from the surface of the nerve tissue relative to the overlying coverslip (reference position) allowed real time measurement of the surface displacement during each laser pulse. An optical trigger facilitated synchronous recording of the exact timing of pulse delivery for all experiments.

To separate the laser-induced temperature effects from stress transients, we investigated the possibility of pulsed stress waves alone leading to a stimulatory effect in neural tissue with a custom-made mechanical piezoelectric element. A piezo actuator (NA-09 Piezo Actuator, DSM, Franklin, TN) with a 9 micron displacement range rated for a total voltage range of $-30/+120$ V was designed and assembled into a structure ($3 \times 1 \times 1$ cm) with a mounting base and location for an output tip. The removable threaded tip insert consisted of a 1 mm diameter fabricated ceramic sphere oriented in the direction of motion of the actuator. This tip design mimicked the shape and size of a Gaussian beam profile similar to that of the Ho:YAG laser using a 600 micron fiber (NA = 0.39) located 0.75 mm from the target tissue just at the surface of the irradiated nerve.

The actuator's open loop displacement versus applied voltage was characterized to produce a controlled velocity move to mimic the surface displacement from DP-OCT data collected using threshold radiant exposures with the Ho:YAG laser (at least 300 nm in 350 μs). The actuator was connected to a linear amplifier (VF-2000, DSM, input voltage gain = 21.3). The entire system was computer controlled by a software program (Labview, National Instruments, Austin, TX). Triangular and sinusoidal input waves corresponding to an increase and decrease in actuator position allowed for fast pressure transients to be delivered to the surface of the sciatic nerve in vivo. The CNAP and CMAP recordings were triggered from the onset of actuator motion to observe any stimulatory effect from expansion and compression waves. The range of displacement amplitudes used (300 nm to 9 μm) mimicked or exceeded measurements of volumetric tissue expansion (see Fig. 4 in Results) and the time for the total displacement was held at 350 μs, the length of the Ho:YAG laser pulse.

Cold frog experiments

Experiments in frog sciatic nerve examined the temperature dependence of stimulation threshold. The frog was chosen as the best model for these experiments due to its cold-blooded nature and ability to maintain nerve conduction over a wide temperature range. The nerve and optical fiber were submerged in saline maintained at temperatures of 0°C and 25°C, respectively. To determine temperature values of the bath, a wire thermocouple (Type E, Chromel/Constantin, Omega Engineering, Stamford, CT) was suspended in the fluid and temperature values were recorded at a rate of 500 Hz using a data acquisition system (Labview, National Instruments, Austin, TX). Time between trials (10 min) allowed for adequate heat diffusion to tissue, and thus we assume the temperature of the bath and the tissue was identical. This also helped minimize tissue dehydration, which can affect the stimulation threshold. A 600 μm fiber coupled to the Ho:YAG laser was placed 0.4 mm from the nerve surface and stimulation thresholds recorded for three trials at each temperature for each nerve ($n = 6$).

Two-dimensional radiometry of irradiated tissue surface

Two-dimensional radiometry was used to observe the irradiated tissue surface temperature profile in both time and space. Fig. 1 illustrates the Indigo Systems infrared (thermal) camera with Phoenix data acquisition system (22). This system helped gather temperature profiles in vivo upon Ho:YAG laser stimulation of the rat sciatic nerve at 2 Hz. A 600 μm fiber was coupled to the laser and held at a constant distance of 0.75 mm from the tissue during all trials. Temperature measurements were taken for 1 s at a sampling rate of 800 fps, while data were normalized and displayed as a function of time and position (x,y). Nerve surface temperature measurements were observed in the two-dimensional plane (10 mm $\times$ 2.5 mm field of view) both during and after the laser pulse with a resolution of 50 μm^2. Measurements over a range of radiant exposures from stimulation threshold to radiant exposures causing thermal changes in tissue (0.3–0.9 J/cm^2) were conducted in hydrated nerve tissue ($n = 18$).

RESULTS

The first part of the Results section is composed of four subsections, each testing a hypothesis generated for the four possible biophysical mechanisms that we postulate as potential means responsible for transient optical nerve stimulation. Three null hypotheses, assuming that optical stimulation is caused by electric field, photochemical, and photomechanical effects, are considered individually in an effort to evaluate each with theoretical and experimental evidence. We then focus on our primary hypothesis that optical stimulation is mediated by a thermal mechanism. We soon realized that this phenomenon is thermally mediated. The second part of this section aims to characterize the nature and magnitude of the absorption-driven temperature change required to facilitate transient optical nerve stimulation.

Electric field effect

To assess whether the electric field within the incident light beam is adequate to directly initiate action potentials, we calculated the magnitude of the field using the typical laser parameters for transient optical nerve stimulation. Maxwell's electromagnetic theory suggests that an inherent electric field exists within laser light, which is associated with the propagation of light itself where the photon velocity is driven by time and space varying electric and magnetic fields (23). Consider the equation

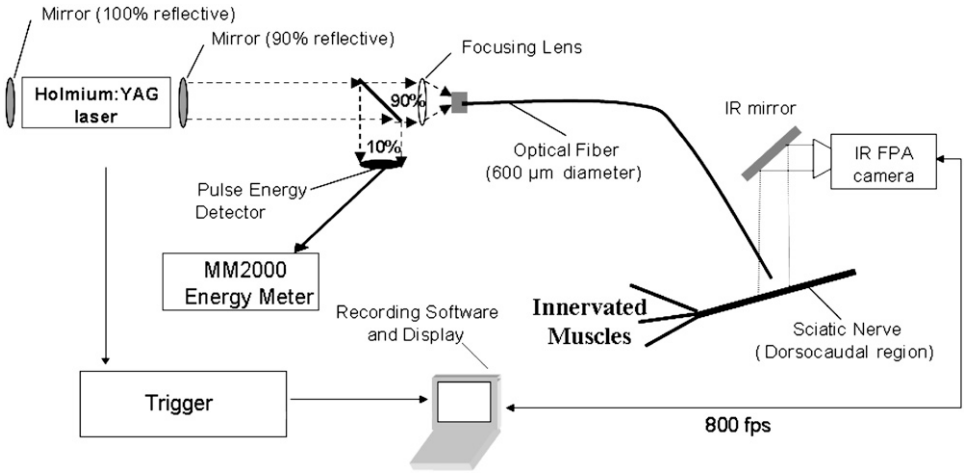

FIGURE 1 Experimental setup for nerve surface temperature measurements with the thermal camera from UTA.

$$S_{\text{threshold}} = 1/2c\varepsilon_o E_{\text{max}}^2, \quad (1)$$

where threshold laser radiant exposure ($S_{\text{threshold}}$) = 0.32 J/cm^2 with the Ho:YAG laser and the product of the speed of light (c) and permittivity of neural tissue (ε_o) equals 0.002634 A-s/V-m (24). The calculated theoretical value for the maximum instantaneous intensity of the electric field (E_{max}) at the tissue surface is 0.155 V/mm^2, predicting that a maximum current of 0.05 mA/mm^2 is delivered to the tissue surface during threshold optical stimulation (R_{total} = 3.1 kΩ). This theoretical prediction is between three and four orders of magnitude below the electrical stimulation threshold for peripheral nerves determined in our previous studies, where 0.95 ± 0.58 A/cm^2 was required for surface stimulation (25). Moreover, it is important to realize that the electric field owing to light oscillates at 10^{14}–10^{15} Hz, which is also orders of magnitude higher than the typical electrical stimulation field oscillator frequency. Calculations based on experimental data predict this stimulation mechanism is unlikely.

To experimentally test the null hypothesis that a light electric field effect causes stimulation, we used the alexandrite laser operating at 750 nm (red light) to attempt excitation of the peripheral nerve. In this setup, laser parameters and beam characteristics remained constant as compared to those of the Ho:YAG laser (i.e., pulse duration, fiber size, spot size, repetition rate, and electric field strength) except for the wavelength, which changed from a fairly high absorption (Ho:YAG, $\mu_a = 3$ cm^{-1}) to a very low absorption (alexandrite, $\mu_a = 10^{-4}$ cm^{-1}) in soft biological tissue. Thus, any stimulation reported was a direct result of the electric field of the laser light, not from absorption-driven photobiological effects. A total of four nerves were irradiated through a range of radiant exposures from stimulation threshold to those causing thermal changes in the tissue (0.3–51.7 J/cm^2). The alexandrite laser did not stimulate the peripheral nerve in any trial using radiant exposures up to 150 times Ho:YAG stimulation threshold. However, using radiant exposures >50 J/cm^2 led to tissue dehydration and a resulting increase in tissue absorption at this wavelength.

Carbonization of the epineurial layer of collagen surrounding the nerve ensued, at which point the laser was able to repeatedly stimulate the nerve. A direct electrical field is highly unlikely as a means for optical stimulation since light from the alexandrite laser did not stimulate at radiant exposures and therefore a maximum electric field, >100 times higher than those used for the Ho:YAG laser. The results from these experiments do support a thermally mediated mechanism (photothermal or photomechanical effects). Heating of the tissue with damaging radiant exposures resulted in stimulation. Carbonization (''burning'') and dehydration of the protective layers surrounding the axons significantly changed the optical and thermal properties of the tissue. In this case the tissue absorption for this wavelength increased and immediately mediated the stimulatory effect. This evidence supports an absorption-driven process as the biophysical mechanism underlying optical stimulation.

Photochemical effects

Photochemical effects from laser irradiation depend on the absorption of light to initiate chemical reactions. Here we consider the null hypothesis that the mechanism for transient optical nerve stimulation is a result of photochemical effects from laser tissue interaction. Theoretically, one can predict that a photochemical phenomenon is not responsible since infrared photon energy (<0.1 eV) is too low to drive direct photochemistry and the applied irradiance is most certainly insufficient for any multiphoton effects (26,27). Previous studies have shown that stimulation threshold exhibits a wavelength dependence based on the absorption coefficient of nerve tissue. Optimal wavelengths have a penetration depth of 300–500 microns; however, all infrared wavelengths with sufficient tissue absorption can cause neural

stimulation. The stimulation thresholds in the infrared part of the spectrum in essence follow the water absorption curve (2), suggesting that no ''magical wavelength'' has been identified. This effectively disproves the notion that a single tissue chromophore is responsible for any direct photochemical effects. This also provides some evidence that the effect is directly thermally mediated or a secondary effect to photothermal interactions (i.e., photomechanical effects) as tissue absorption from laser irradiation can be directly related to the heat load experienced by the tissue.

Photomechanical effects

This phase of the study examined conceivable photomechanical effects leading to optical stimulation, namely pressure wave generation from rapid heating (i.e., thermoelastic expansion and stress wave generation). Contributions from pressure waves to optically stimulate the peripheral nerve were studied by observing the effect of pulse duration on stimulation threshold. Fig. 2 depicts the effect of varying pulse width on the minimum incident radiant exposure required for action potential generation using three lasers with nearly equivalent absorption coefficients but varying pulse durations. The corresponding penetration depths from the Ho:YAG (2.12 μm, 350 μs), FEL (2.1 μm, 5 μs), and tunable solid-state diode laser (1.87 μm, 1–5 ms) were 330, 333, and 450 μm, respectively. Hence, stimulation threshold was established for five different pulse durations (5 μs, 350 μs, 1 ms, 3 ms, 5 ms) for 10 trials each. This figure demonstrates that the threshold radiant exposure required for stimulation at this tissue absorption does not change with variable pulse width through almost three orders of magnitude. Based on theoretical calculations and experimental data collected during optical stimulation using a hydrophone (data not shown), the induced change in pressure is <1 bar.

Photomechanical effects produce forces, such as explosive events and laser-induced pressure waves, which can impact cells and tissue. Since we are operating well below the ablation threshold, ablative recoil can be excluded as a source of mechanical effects. Nerve stimulation using pressure waves (rapid mechanical displacement, ultrasound) is well documented in the literature (28,29). The relationship between laser penetration depth and pulse duration provides critical information concerning confinement of the laser energy in both space and time. Fig. 3 is a well-known graph in tissue optics that depicts the relationship between these two laser parameters to define theoretical zones separating stress confinement, thermal confinement, and no confinement of the laser pulse. The results provide experimental data that discount the possibility of pressure wave generation from rapid heating leading to optical stimulation. The three lasers used in the comparison between pulse duration and stimulation threshold (Fig. 2) are labeled in Fig. 3.

Note that each of these lasers resides in the thermally confined regime, or the pulse width is adequately short to curtail heat diffusion during the pulsed energy deposition. Similarly, the pulse width is satisfactorily long, such that laser-induced stress effects and pressure wave propagation are minimal. If we assume some level of pressure transients are generated in tissue and these waves result in tissue stimulation, then we would expect the stimulation threshold to decrease (i.e., it becomes easier to stimulate using the FEL 5 μs pulse) the closer a laser lies to the stress confinement zone. However, we clearly see the difference in threshold radiant exposures is not significant over three orders of magnitude change in pulse duration with equivalent penetration depths across the thermal confinement zone. Pressure waves attributable to thermoelastic expansion or stress wave propagation are not generated in tissue with these experimental parameters for optical stimulation and do not contribute to excitation. In contrast, volumetric expansion will always

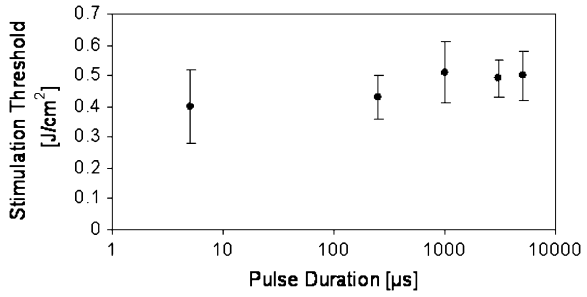

FIGURE 2 Effect of laser pulse duration on stimulation threshold radiant exposure. Three lasers with comparable tissue absorption coefficients were used: the FEL (5 μs), Ho:YAG (350 μs), and tunable solid-state pulsed diode laser (1, 3, 5 ms). All lie well outside stress confinement but are still thermally confined.

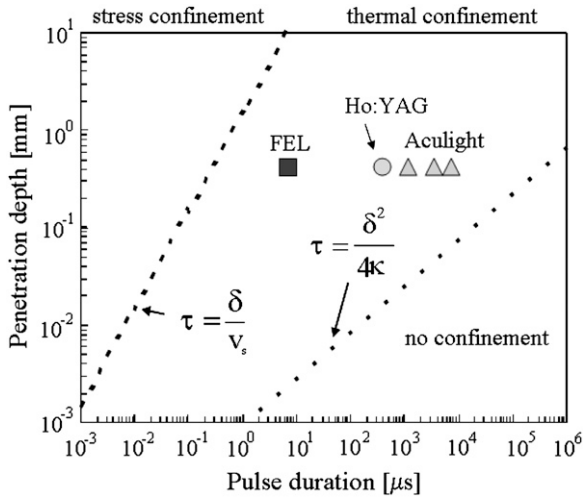

FIGURE 3 Confinement zones based on penetration depth and pulse length for soft tissue. Notice that the three lasers used are all thermally confined but are not stress confined. (Reprinted, modified version of Fig. 13 from Jacques, S. L. 1992. Laser-tissue interactions. Photochemical, photothermal, and photomechanical. Surg. Clin. North Am. 72:531–558, with permission from Elsevier.)

result from heating tissue since a higher temperature will result on average in larger molecular spacing.

Volumetric expansion of the nerve surface was measured during the laser pulse using a phase-sensitive OCT setup (at UTA) over the typical range of radiant exposures required for peripheral nerve excitation to determine tissue displacement upon light absorption and subsequent tissue heating. The typical nerve displacement in time measured from this system during a single laser pulse is seen in Fig. 4 (*right*). The maximum increase in optical path length change of the waveform corresponds to the immediate absorption, heating, and maximum expansion resulting from the laser pulse. The time required for the maximum displacement to occur is 350 μs, which is exactly the duration (FWHM) of the Ho:YAG laser pulse. The exponential decay in displacement represents the typical thermal decay in tissue based on the thermal diffusion time, a tissue property. Fig. 4 (*left*) describes the maximum change in surface displacement of three rat sciatic nerves (ex vivo) upon irradiation with Ho:YAG laser over the typical physiologic range of radiant exposures for optical stimulation. As expected, displacement increases linearly with laser radiant exposure, theoretically supported by the following equation:

$$\Delta T = (1/b)(\Delta V/V), \tag{2}$$

where the change in temperature (ΔT) is linearly proportional to the ratio of the change in volume (ΔV) over the total irradiated initial tissue volume (V) and related by the product of the inverse of the volumetric expansion coefficient (b in units [K^{-1}]). Surface displacement near threshold (0.4 J/cm^2) was measured to be 300 nm.

Quantitative data on the exact amplitude and duration of the pressure transients secondary to tissue temperature changes from pulsed laser irradiation were used to design a piezoelectric actuator that mimicked beam characteristics in optical stimulation. The actuator tip was constructed to correspond to the laser spot size used in DP-OCT experiments, which normalized the effective tissue volume changes upon tissue displacement (see Eq. 2) between these two sets of experiments. Here displacements from tissue volume changes are detached from temperature increases to examine the effect, if any, from simulated photomechanical stimulation of the peripheral nerve. A variety of mechanical pulse wave shapes and amplitudes were delivered to a total of 10 rats (20 nerves). For each nerve, both triangle and sinusoidal-shaped waveforms varying in amplitude from 300 nm to 9 microns were delivered normal to the surface of the nerve via the beam-shaped actuator tip. Based on results from displacement measurements in Fig. 4 (*right*), the maximum temperature rise occurs 350 μs after onset of the laser pulse (the pulse width of the Ho:YAG). Compression and expansion waveforms were delivered in this 350 μs time course for all experiments. We see no evidence suggesting that pressure transients analogous to laser-induced volumetric expansion waves can initiate action potentials with amplitudes at least 30 times those measured for optical nerve stimulation threshold.

Although it is possible that pulsed laser irradiation induces pressure transients in the target tissue owing to the volumetric expansion effect, the contributions of this to optical stimulation are expected to be minimal with the laser parameters used. The pulse duration of 350 μs exceeds the stress confinement time for this wavelength by nearly three orders of magnitude, resulting in a dissipation of thermally induced pressure during the laser pulse and consequently little pressure buildup (30,31). The results from DP-OCT surface displacement measurements support this notion and identify the exact relationship between laser radiant exposure and the subsequent upper limit in magnitude of expansion in nerve tissue. Results from the successive piezoelectric actuator

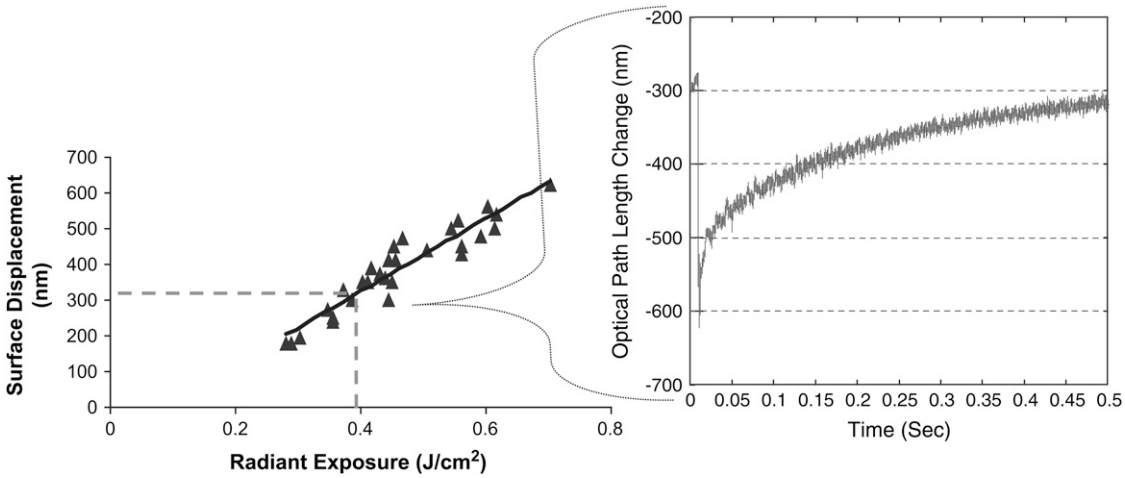

FIGURE 4 DP-OCT measurements of nerve surface displacement resulting from Ho:YAG laser irradiation. (*Right*) Typical recording of the optical path length change of the nerve surface relative to a stationary coverslip from near threshold radiant exposure (0.4 J/cm^2) indicating volumetric tissue expansion on the order of 300 nm. (*Left*) A total of 18 measured surface displacements over the normal range of use for optical stimulation radiant exposures ($R^2 = 0.8951$).

experiments reveal that pressure transients delivered to the nerve surface in a manner analogous to laser-induced expansion waves are not capable of initiating action potentials with amplitudes at least 30 times those measured for optical nerve stimulation threshold. These experiments provide compelling evidence that temperature-induced volumetric expansion is trivial for radiant exposures much greater than threshold and indicate that the mechanism lacks photomechanical contributions.

Photothermal effects

Through this null hypothesis approach to divulge the mechanism responsible for transient optical nerve stimulation, we have shown electric field, photochemical, and photomechanical effects from laser tissue interactions do not result in excitation of neural tissue. Preliminary evidence related to the thermal nature of the biophysical mechanism lies in results from the alexandrite laser stimulation of the peripheral nerve. As optical and thermal properties in the tissue changed upon tissue dehydration, the absorption of the alexandrite increased and a subsequent decrease in stimulation threshold radiant exposures was reported. Thus, we have arrived at the hypothesis that laser stimulation of nerves is mediated by some absorption-driven photothermal process resulting from transient irradiation of peripheral nerves using infrared light. We will now present supporting evidence for this claim. We will then precisely quantify the spatial and temporal thermal transients after optical stimulation of peripheral nerve over the physiologically valid range of radiant exposures implemented with this methodology.

The effect of pulse width changes on the onset time for stimulation and action potential propagation was observed. Nerve potentials were recorded exactly 6 mm distal to the site of rat peripheral nerve stimulation using the Aculight pulsed diode laser ($\lambda = 1.87\ \mu$m). Fig. 5 depicts the recorded CNAPs using 2.5 ms and 8.0 ms laser pulse widths in the same nerve. The recording site and stimulation site as well as all additional laser parameters were constant for results shown in Fig. 5, *a* and *b*. A laser radiant exposure slightly above threshold was maintained constant for each recording (0.4 J/cm^2), evidenced by the similar peak CNAP amplitudes. Both pulses delivered the same amount of total energy, yielding a difference in power delivered (i.e., the power delivered with the 2.5 ms pulse was 3.2 times higher than that in the 8 ms pulse). Similar motor axons were recruited for each trial, thus it is reasonable to assume that the conduction velocities for the recordings in Fig. 5, *a* and *b*, are identical. This yields a conduction time from the site of stimulation to recording of 2.6 ms for the CNAPs in Fig. 5. The onset time for stimulation varies with width of the laser pulse. We can surmise that all laser energy must be deposited in the tissue before an action potential is generated. This implies that, in the absence of pressure transients, the tissue must sustain some minimal thermal change before excitation of the underlying axons can occur. These results further illustrate the importance of pulse width in optical stimulation—predicting that longer pulses will increase the time required for an evoked CNAP and decrease the probability of stimulation due to onset of thermal diffusion in tissue.

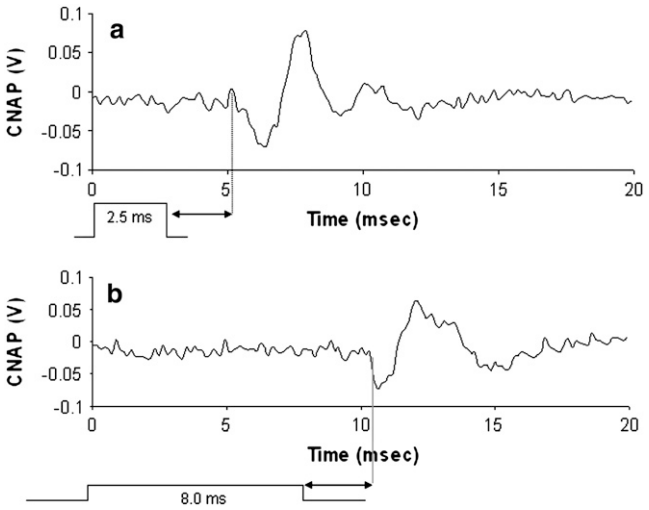

FIGURE 5 CNAP signal onset time for two different laser pulse durations. Assume the time for conduction over 6 mm from stimulation site to recording electrodes is constant (2.6 ms, *arrows*) after the pulse energy deposition. (*a*) CNAP recorded from stimulation at $t = 0$ using a 2.5 ms pulse duration with the pulsed diode optical nerve stimulator. (*b*) CNAP recorded from stimulation at $t = 0$ using a 8.0 ms pulse duration with the pulsed diode optical nerve stimulator. These recordings prove that all laser energy is required before the onset of the CNAP can occur (Gain = 5000).

A thermally sustained mechanism naturally introduces a query as to the nature of the temperature change required in the tissue. We begin to build this understanding by questioning whether this stimulatory thermal change requires a minimum absolute value or rather a thermal gradient, a time-dependent temperature change. Results discussed to this point validate either claim; however, data collected regarding temperature dependence on stimulation threshold help to make this distinction. The effect of nerve tissue temperature on the threshold radiant exposure required for stimulation was determined using the frog sciatic nerve model. The cold-blooded amphibian nerve temperature was manipulated in a saline bath in vivo to facilitate nerve stimulation at temperatures of 0°C and 25°C. Both the optical fiber for stimulation and the peripheral nerve were submerged in the temperature-controlled saline solution and held at a distance 0.4 mm away from the target tissue. This caused the reported threshold radiant exposures for stimulation to increase as the saline between the fiber and tissue absorbed much of the optical energy. Since this is a comparative study all experimental parameters remained unchanged for each trial to normalize collected threshold data. Stimulation threshold averages at 25°C were 0.91 and 0.84 J/cm^2 for the two frogs studied with

three trials for each nerve ($n = 6$). Similarly, average thresholds for stimulation at 0°C were 1.01 and 0.86 J/cm^2 ($n = 6$), respectively.

Results from the threshold dependence on nerve tissue temperature experiments indicate no statistically significant change ($p < 0.05$) in threshold radiant exposures occurs (maximum change of 6%) with changes in nerve tissue temperature. This is despite the fact that a tissue temperature change of 25°C in the nerve-air interface experimental setup requires a radiant exposure of at least 1 J/cm^2 (see Fig. 8). In other words, the radiant exposures necessary for a 25°C change the saline submerged nerve interface experimental setup (i.e., frog temperature experiments) would require at least 100% more laser energy used for stimulation. In contrast, the measured stimulation thresholds are not significantly different across a large tissue temperature range, varying by an average of 6% between trials. From these results we can conclude that at least in the frog there is no set threshold tissue temperature that must be reached to initiate the action potential, as the threshold for optical stimulation does not change with large tissue temperature differences upon laser pulses associated only with small increases in tissue temperature. This was further confirmed in an experiment where we compared the onset time of stimulation for two different laser radiant exposures using an identical laser pulse width. In this scenario it was discovered that a nerve potential is induced as soon as a given amount of energy is deposited in the tissue or a proportionally earlier onset for the higher radiant exposure case. Again this provides experimental proof that the radiant exposures greater than threshold will initiate action potentials before completion of the laser pulse, indicating propagation will begin as soon as the temperature rise required for excitation (threshold temperature at the axonal membrane) is reached. Thus, the mechanism for optical stimulation is a temperature-dependent and transient phenomenon requiring a certain increase in temperature in a given short time (i.e., the laser pulse width).

Characterization of the thermal gradient

The data presented indicate that the mechanism responsible for transient optical nerve stimulation is an absorption-driven photothermal effect that specifically requires a temperature rise at the nerve axon level to initiate action potential generation. Photothermal effects include a large group of interaction types resulting from the transformation of absorbed light energy to heat, leading to a local temperature increase and thus a temperature gradient both in time and in space. It is essential to emphasize that thermal interactions in tissue are typically governed by rate processes, where both the temperature and time are parameters of major importance. Heat flows in biological tissue whenever a temperature difference exists according to the laws of thermodynamics. The primary mechanisms of heat transfer to consider include conduction, convection, and radiation (32). The data imparted in the following section help detail and quantify the spatial and temporal gradients required for optical nerve stimulation.

Two-dimensional radiometry of the irradiated tissue surface was performed with the thermal camera to gain a better understanding of thermal processes and actual tissue temperature values needed for optical nerve stimulation. The temperature profile in space and time were observed after Ho:YAG laser stimulation. Fig. 6 represents the surface temperature profile (x,y) of a single frame containing the maximum temperature value recorded for all frames (800 fps recording) irradiating the nerve with threshold radiant exposure (0.4 J/cm^2) or immediately after the end of the laser pulse. This corresponds to the first frame in which all laser energy has been deposited into the tissue. Temperature profile for the column (*right*) and row (*left*) containing the maximum temperature pixel are shown below. Solid lines represent the best Gaussian fit for each temperature profile. Peak tissue temperature for this trial upon optical nerve stimulation in vivo (well-hydrated tissue with room temperature saline baseline temperature of 26.91°C) was measured to be 35.86°C. This is a peak temperature rise of 8.95°C, yielding an average temperature rise across the Gaussian laser spot of 3.66°C with radiant exposures near stimulation threshold. This is very close to the theoretically calculated average temperature rise for a uniform beam with the same laser parameters and neglecting scattering equal to 2.87°C (25).

Thermal measurements of the rat sciatic nerve surface ($n = 18$) were taken in vivo for each nerve using a range of radiant exposures 0.3–0.9 J/cm^2 in well-hydrated tissue. Fig. 7 *a* represents the data collected for the maximum surface temperature for a single trial (*diamonds*) and peak temperature rise in tissue (*squares*) immediately after laser stimulation as a function of radiant exposure. Fig. 7 *b* describes the average thermal gradient, temperature rise from baseline, as a function of laser radiant exposure for all trials ($n = 18$). As expected, nerve temperature increases linearly with laser radiant exposure. Results predict the minimum temperature increase of the nerve surface required for stimulation (0.3–0.4 J/cm^2) is as low as 6°C, yielding a peak temperature of 31°C, provided that the laser pulse width is sufficiently short (<10 ms based on previous experiments). Minimum temperatures for onset of thermally induced changes in mitochondria function and protein denaturation are shown in Fig. 7*a*. In the case of nonhydrated tissue (data not shown), the temperature as a function of radiant exposure shifts upward due to a difference in optical and thermal properties compared with higher water content tissue. Here the mitochondrial damage will theoretically begin to occur between 0.5 and 0.6 J/cm^2, thus illustrating the importance of tissue hydration for safer, more efficient nerve excitation.

The peripheral nerve temperature profile in time was also observed using the infrared camera. Fig. 8 shows the results from Ho:YAG laser stimulation slightly above threshold

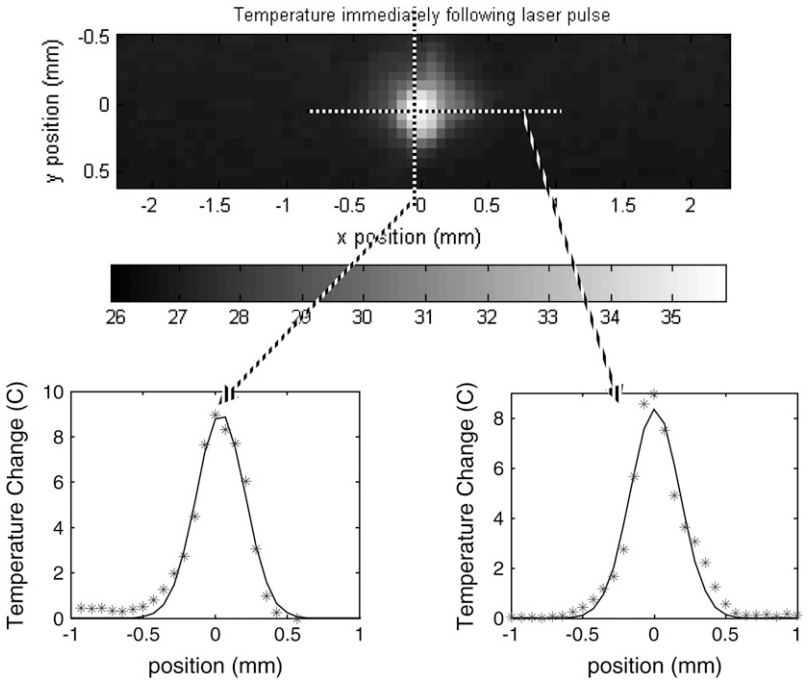

FIGURE 6 Temperature spatial profile measurement of the nerve surface in vivo using the thermal camera at the end of the laser pulse. Threshold (0.4 J/cm^2) radiant exposure with a 600 μm fiber yields a peak tissue temperature = 35.86°C, peak temperature rise = 8.95°C, and average temperature rise = 3.66°C. The calculated Gaussian spot = 0.37 mm^2. The position of the maximum pixel for 0.4 J/cm^2 stimulation (*stars*) and Gaussian fit (*solid line*) of temperature profile for maximum line scan in x and y are shown.

(0.4 J/cm^2) and at two times threshold radiant exposure (0.8 J/cm^2). These graphs provide the peak temperature at the height of the Gaussian spatial profile for each frame in time after a single laser pulse at $t = 0$. The exponential decrease of temperature in time represents a typical thermal decay. Thermal relaxation time (i.e., the time to dissipate heat absorbed from a laser pulse) is defined as the time for the temperature of the tissue to return to 1/e (37%) of the maximum tissue temperature change. In the case of the rat peripheral nerve, based on Fig. 8 we estimate the thermal relaxation time to be ~90 ms. The theoretically calculated value for thermal diffusion (or relaxation) time is equal to 170 ms in soft tissue ($\tau_{th} = \delta^2/4\alpha$) assuming only axial diffusion (33). Since some radial diffusion will occur given the spot size/penetration depth ratio in this experimental setup, the actual value is expected to be less than this value; and indeed this is true in actual measured values. As expected, the thermal relaxation time is independent of laser radiant exposure.

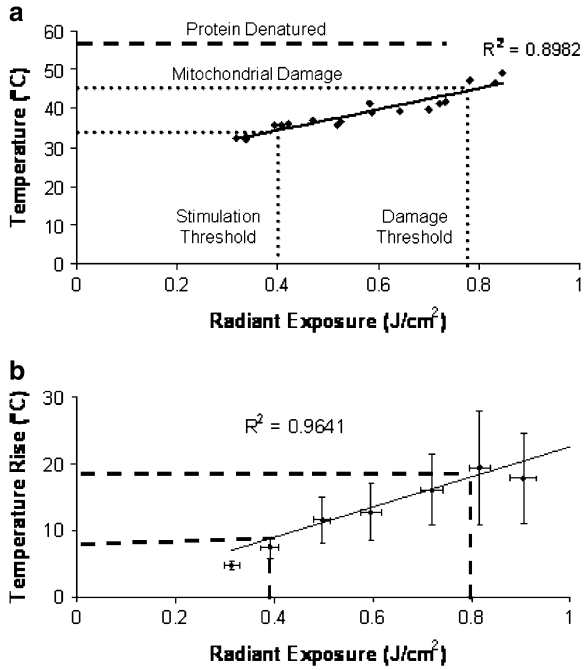

FIGURE 7 (*a*) Maximum temperature in hydrated tissue as a function of radiant exposure immediately after laser stimulation. Stimulation threshold occurs between 0.3 and 0.4 J/cm^2; onset of minimal thermal changes in tissue occurs at 43°C, which corresponds to the onset of thermal damage seen in previously published histological analysis (0.8–1.0 J/cm^2). (*b*) Average temperature rise from multiple trials ($n = 18$).

Temperature superposition, or additive temperature effects from multiple pulses, was observed for a period of 5 s using 2 Hz and 5 Hz stimulation frequencies. These results are shown in Fig. 9. It is clear that the temperature increase and return to baseline tissue temperature is consistent upon multiple laser pulses with a frequency of 2 Hz regardless of laser radiant exposure. This demonstrates that there are no additive temperature effects in peripheral nerve tissue with low frequency stimulation near threshold. A frequency of 5 Hz does have temperature superposition effects as the tissue temperature increase does not return to baseline before absorption and heating from the next pulse in the sequence. This quickly leads to a much larger maximum temperature in the tissue than seen with 2 Hz stimulation. A larger radiant exposure will result in more pulses required to reach a maximum temperature steady state as more thermal energy must dissipate to surrounding tissue through heat conduction.

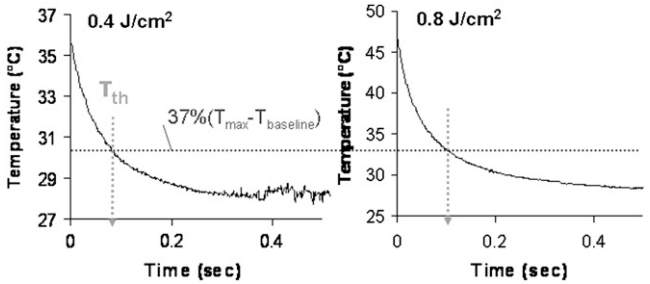

FIGURE 8 Temperature profile of peripheral nerve in time, laser stimulation near threshold (0.4 J/cm^2), and at over 2 times threshold (0.8 J/cm^2). The experimental thermal relaxation time, τ_{th}, of peripheral nerve tissue based on the equation shown in the figure is 90 ms.

DISCUSSION

Optimal laser parameters and characteristics for efficient stimulation

The finding that a thermal gradient in the target nerve is the underlying biophysical mechanism for excitation combined with knowledge of the extent of these temperature rises affords insight into some fundamental limitations and optimal parameters for appropriate use of this technique. First, we can draw some conclusions on spatial selectivity. It is somewhat surprising that the temperature profile follows a Gaussian distribution in space (Fig. 6) with such a small optical fiber to tissue distance (0.5 mm), since Verdaasdonk and Borst (34) have shown a more uniform beam shape at this distance. Thus, the spot calculated using the angle of light divergence from the fiber (NA = 0.39, divergence = 23°) assuming a uniform beam (~1 mm^2) is actually a larger estimation than the Gaussian spot size measured here (0.37 mm^2). Assuming a specific temperature rise is responsible for action potential generation with pulsed light, the effective stimulation area must occur within a very small spot where the peak temperature change within the tissue is high.

We can infer from the temperature change versus position graphs in Fig. 6 that near threshold the effective stimulation diameter is confined to the tip of the Gaussian curve, on the order of 200 μm or less. This validates the superior spatial precision seen with transient optical nerve stimulation and the technique's ability to excite discrete populations of axons within individual nerve fascicles. Note the optical fiber size used in these experiments has a 600 μm diameter; therefore the affected tissue area is actually smaller than the size of the fiber and obviously significantly smaller than the zone of irradiated tissue (Gaussian temperature profile). If the laser energy is increased, a greater tissue radius will overcome the required temperature rise threshold. As a result, the selectivity will ultimately decrease as a greater area (thus greater number of axons) will be excited by the incident laser beam. Theoretically, the minimum spot size for optical stimulation is limited only by light diffraction and no doubt can be delivered to tissue via optical fibers as small as 4 μm.

Second, we infer an upper limit to the range of nondamaging laser radiant exposures for low frequency optical stimulation. The literature suggests that thermal changes to mitochondria may begin to occur with temperatures as low as 43°C (35,36), whereas protein denaturation begins at tissue temperatures close to 56°C–57°C (16). As shown in Fig. 7, this temperature corresponds to an onset of thermal changes in peripheral nerve connective tissues with radiant exposures as low as 0.75 J/cm^2, whereas thermal damage to the actual underlying axons will require laser energies greater than this value based on the exponential attenuation of light in tissue. These results support the reported tissue damage threshold radiant exposures determined from histological analysis of

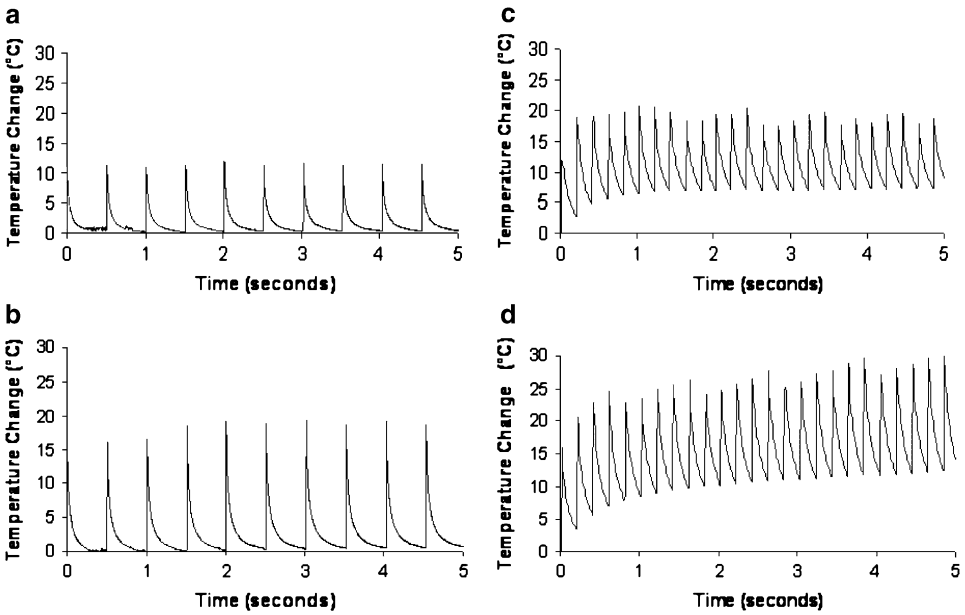

FIGURE 9 Steady-state maximum temperature increase in nerve tissue from Ho:YAG laser stimulation. (*a*) Temperature rise from 0.45 J/cm^2 radiant exposure pulses at 2 Hz stimulation frequency. (*b*) Temperature rise from 0.65 J/cm^2 radiant exposures at 2 Hz stimulation frequency. (*c*) Temperature rise from 0.41 J/cm^2 threshold radiant exposures at 5 Hz stimulation frequency. (*d*) Temperature rise from 0.63 J/cm^2 threshold radiant exposures at 5 Hz stimulation frequency.

short-term laser nerve stimulation (0.8–1.0 J/cm^2) (2). Owing to the fact that the nerve is exposed through an open incision and hydrated with room temperature saline (baseline temperature = 27°C), the maximum temperature rise at threshold is still below normal body temperature (36°C) and therefore well below temperatures required for thermal changes or tissue damage. These results imply that optical stimulation of motor axons in peripheral nerves is mediated through surface thermal gradient of 6°C–10°C temperature rises, whereas this gradient has both temporal (see Fig. 8) and spatial (see Fig. 6) components.

These temperature changes may be an overestimate in actual temperatures required for threshold excitation, as our endpoint is a functional muscle contraction requiring recruitment of multiple axons to elicit a visible response. In fact, published work on the stimulation of the cochlear nerve, lacking epineurial sheaths, demonstrates stimulation threshold radiant exposures are two orders of magnitude smaller than those reported here in the peripheral nerve (37). Furthermore, these results indicated that this phenomenon is theoretically nondamaging in peripheral nerve tissue with radiant exposures at least two times the threshold required for action potential generation. Since a change in tissue temperature, as opposed to an absolute temperature, is implicated as the mechanism of action, cooling of the tissue before irradiation may improve the safety of this technique by minimizing the maximum temperature achieved during stimulation.

Third, we surmise the upper limits for repetition rate without leading to superposition of temperature in tissue upon multiple pulses. Looking at Fig. 9 one can deduce that temperature superposition will begin to occur at higher repetition rates (>4–5 Hz) as the tissue requires slightly >200 ms to return to baseline temperature. At repetition rates >5 Hz tissue temperatures will become additive with each ensuing laser pulse, and resulting tissue damage may begin to occur with prolonged constant stimulation. This assumption is supported by the results shown in Fig. 9. With low-frequency stimulation (Fig. 9 *a*) the resultant heat load in tissue after the laser pulse has adequate time to diffuse out of the irradiated zone via heat conduction. Alternatively, higher frequency stimulation is clearly marked by temperature superposition as additional pulses become additive to the overall tissue temperature. Conduction is overcome by the frequency of laser pulses, and within 5–10 pulses a steady state temperature and baseline are achieved. According to the results shown in Fig. 6 *a* damage will occur with changes between 18°C and 20°C. Temperature increases greater than those recorded in the high frequency stimulation experiment are approaching this upper limit using threshold value radiant exposures. Fig. 9 *b* plainly shows that the upper limit for the frequency of optical stimulation is 5 Hz in the peripheral nerve. Neural tissues with lower threshold radiant exposures for stimulation will tolerate significant increases in the maximum repetition rate limits.

Finally, we can conclude the maximum laser pulse duration for practical use of this technique in peripheral nerve stimulation. There is strong evidence against laser-induced pressure waves underlying the optical stimulation mechanism (the pulse duration is too long to facilitate stress confinement, and indeed negligible stress transients were measured), and no significant difference was found in stimulation thresholds from the three laser sources, despite a 1000-fold difference in pulse duration. Given this information, it is plausible to assume that stimulation is not dependent on the pulse duration provided the pulse is short enough to minimize heat diffusion during the laser pulse (i.e., conditions of thermal confinement are fulfilled). Although theory predicts that the pulse length may be stretched up to hundreds of milliseconds before no confinement is achieved (see Fig. 3), experimentally this is an overestimate. Heat diffusion begins immediately (see Fig. 9), which causes the quality of the evoked potentials to be significantly diminished with laser pulse widths >10 ms. Pulses delivered in a time less than this value result in crisp potentials with every pulse; however, pulses longer than 10 ms tend to have a more intermittent and indolent response. In the case of motor axon stimulation, this functionally presents as an irregular and disjointed muscle contraction as opposed to a fast, reliable twitch with shorter laser pulse durations.

Defining the thermal gradient for transient optical nerve stimulation

Photothermal interaction leading to temperature increase is highly dependent on the optical properties of the nerve, such as absorption and scattering coefficient, and thermal properties, such as thermal conductivity and specific heat (38). In the infrared, the diameter of the sciatic nerve is much larger when compared with the penetration depth of the light stimulus employed. This implies that all light energy that enters the tissue is trapped inside except losses from diffuse reflection from the nerve surface. Absorption coefficients are very high compared to the effective scattering in this wavelength range because soft tissue is dominated by forward scattering ($g \sim 0.9$) (39). Therefore absorption alone is the significant factor for interaction of the laser light with tissue, and scattering plays a negligible role in the light distribution and resulting light-induced effect on the nervous tissue. To calculate the percentage of surface temperature that reaches the axonal layer in peripheral nerve we employ Beer's Law and make the following assumptions: 1), absorption dominated laser penetration ($\mu_a(\lambda = 2.12) = 3\ \text{mm}^{-1}$); 2), peripheral nerve connective tissue (epineurium, perineurium, endoneurium) is a homogenous tissue; 3), the average thickness of the layers surrounding the axonal layer is 150 μm; 4), the minimum surface temperature rise required for optical stimulation is 6°C–10°C; and 5), the percentage of light attenuation is equal to the percentage of temperature attenuation in a single layered medium.

These assumptions predict that 63.8% of the light entering the peripheral nerve surface will remain at the average depth of the axonal layer for selective stimulation of a specific fascicle. Thus, the temperature rise required at the surface of the Schwann cells (myelination) surrounding the axonal membrane that results in optical stimulation of neural tissue is ~3.8°C–6.4°C. We argue that all types of neural axons can be optically stimulated with the use of optimal laser parameters based on tissue structure and morphology. However, it is important to understand that some physical substance (i.e., connective tissue) to hold the thermal gradient may decrease the radiant exposure needed to facilitate neural excitation. Therefore, to selectively excite central neurons, in vivo or in culture in a large bath medium, may require one or more of the following laser parameter changes: 1), a greater radiant exposure than reported here; 2), a shorter pulse width laser due to much faster thermal diffusion in this tissue type and preparation; 3), an exogenous chromophore; or 4), a specific wavelength targeting substances that lie close to the axonal membrane to establish the necessary thermal gradient and cause the desired stimulatory effect.

Possible physiological stimulation mechanisms from a thermal gradient

It is well known in electrical stimulation that membrane depolarization occurs at the cathode where the concentration of negative potential, or charge density, reduces the potential difference across the membrane, subsequently activating voltage-gated ion channels leading to a transmembrane current from capacitive conductance and action potential propagation (40). The results presented here both imply that a temperature rise leading to a thermal gradient is established at the axonal membrane level upon pulsed laser irradiation and provide evidence that this type of microscale thermal interaction is the biophysical mechanism of optical nerve stimulation. Information on the biophysical mechanism can now help guide experimental research in pursuit of a physiological mechanism at the membrane level. The microscopic heating effects taking place at the cellular level, such as the heating of cellular organelles or changing of channel-gating kinetics, are not verified through these experiments; however, we offer some reasonable explanations for this photobiological phenomenon.

Temperature can affect action potential propagation in three ways: 1), the Nernst equilibrium potentials are inversely proportional to the absolute temperature; 2), the conductance of an open ion channel is dependent on a common temperature factor governing the rate for channel induction called a Q10; and 3), a change in temperature changes the amplitude and duration of the potential (41). One hypothesis for the physiological mechanism for optical stimulation involves sodium channel activation based on a local increase in the conductance as the channel transitions to the open state resulting from a temperature increase. We assume that this is a plausible candidate since sodium channels typically initiate the onset and propagation of a potential in a stimulated axon. Note here that only a threshold potential must be reached by the temperature gradient. Once the inward sodium current is established, it further decreases the membrane potential and drives the generation of the action potential. These channels have known Q10 values; therefore, the conductance of the open channel is temperature dependent. Transient heating from laser energy may result in an increase in overall conductance with temperature, which could result in an inward current. In fact, it is well known that temperature jumps in single nodes of Ranvier result in shifts in membrane potential from charge redistribution and associated membrane currents (42,43). The current density, based on the number of channels open per unit area in a large myelinated axon, over the irradiated area (i.e., a node of Ranvier) may produce the current sufficient to create the localized voltage gradient needed to activate sodium channels and result in regenerative action potential propagation. The requirement for transient delivery of laser energy for optical stimulation supports this theory.

A second potential hypothesis is the activation of heat-sensitive channels, where the gating mechanism is markedly different from the other channel types: voltage-gated, ligand-gated, and mechanosensitive ion channels. A review of the known ion channels gated by heat is given by Cesare et al. (44), who suggest that this temperature rise causes the heat-sensitive channels to change to a more disordered state (45,46). These channels can undergo sensitization, which causes a shift in the relationship-linking temperature to the probability that a channel is open toward a lower temperature (47). This may explain the reason a temperature rise and not an absolute temperature is required for activation. The known heat-sensitive channels responding to increase in temperature all have extremely large Q(10) values (>10) (48–50). Predictions on likely channel candidates for targeted optical stimulation will require more scientific investigation of the existence of heat-sensitive channels in efferent fibers or a new channel type responsive to the thermal stimulation parameters reported here.

Hirase et al. from the Rafael Yuste lab at Columbia University reported depolarization and subsequent action potential firing in transiently irradiated pyramidal neurons with a high intensity mode-locked near infrared femtosecond laser (27). These methods caused cell damage and are markedly different (i.e., damaging, high energy) from the nerve stimulation technique discussed here. Regardless, they offer two mechanisms, including photochemical reaction producing reactive oxygen species adjacent to the cell membrane as well as transient, reversible membrane poration from perforation of tissue light interaction. We disagree with these mechanisms with regard to our methodology for transient optical nerve stimulation, and in this work have shown that this mechanism is not mediated through photochemistry. We anticipate that this stimulation outcome is a

direct effect on transmembrane proteins in the membrane and not a localized reversible pore which would require a large energetic magnitude to separate the lipid bilayer.

CONCLUSIONS

The results presented here reveal that neural activation with pulsed light occurs by a transient thermally mediated mechanism. The electric field effect, photochemical means, and photomechanical mechanisms are discarded as possible means for activation of nerve potentials. Data collected reveal that the spatial and temporal nature of this temperature rise, including a measured surface temperature change required for stimulation of the peripheral nerve (6°C–10°C) and at the axon level (3.8°C–6.4°C). This information has been used to detail the limits in selectivity, pulse duration, and repetition rate using this technique in the peripheral nerve. Ultimately, we envision that this information will form the basis for the development of a portable, handheld device for optical stimulation based on solid-state diode laser technology, operating at the optimal laser parameters to incite a safe and effective motor response. Such a device would have utility in both basic electrophysiology studies as well as clinical procedures that currently rely on electrical stimulation of neural tissue. Our group has recently started collaboration with a commercial laser company (Aculight, Bothel, WA) to explore the use of infrared diode lasers for this purpose.

The authors thank C. Rylander and B. Chen from the University of Texas in Austin for their help with the infrared camera and PS-OCT measurements. We also thank Dr. Robert Macdonald from the neurology department at Vanderbilt University for his guidance regarding the underlying cellular mechanisms that may contribute to stimulation.

This research was supported by the Medical Free Electron Laser center grant FA 9550-04-1-0045 funded through the Air Force Office of Scientific Research and the National Institutes of Health grants R01 NS052407-01 and R43 NS051926-01.

REFERENCES

1. Wells, J. D., C. Kao, E. D. Jansen, P. Konrad, and A. Mahadevan-Jansen. 2005. Application of infrared light for in vivo neural stimulation. *J. Biomed. Opt.* 10:064003.
2. Wells, J. D., C. Kao, K. Mariappan, J. Albea, E. D. Jansen, P. Konrad, and A. Mahadevan-Jansen. 2005. Optical stimulation of neural tissue in vivo. *Opt. Lett.* 30:504–507.
3. Jacques, S. L. 1992. Laser-tissue interactions. Photochemical, photothermal, and photomechanical. *Surg. Clin. North Am.* 72:531–558.
4. Chung, M. K., A. D. Guler, and M. J. Caterina. 2005. Biphasic currents evoked by chemical or thermal activation of the heat-gated ion channel, TRPV3. *J. Biol. Chem.* 280:15928–15941.
5. Orchardson, R. 1978. The generation of nerve impulses in mammalian axons by changing the concentrations of the normal constituents of extracellular fluid. *J. Physiol.* 275:177–189.
6. Quasthoff, S. 1994. A mechanosensitive K^+ channel with fast-gating kinetics on human axons blocked by gadolinium ions. *Neurosci. Lett.* 169:39–42.
7. Yamamoto, M., T. Nagano, I. Okura, K. Arakane, Y. Urano, and K. Matsumoto. 2003. Production of singlet oxygen on irradiation of a photodynamic therapy agent, zinc-coproporphyrin III, with low host toxicity. *Biometals.* 16:591–597.
8. Takahashi, M., T. Nagao, Y. Imazeki, K. Matsuzaki, and H. Minamitani. 2002. Roles of reactive oxygen species in monocyte activation induced by photochemical reactions during photodynamic therapy. *Front. Med. Biol. Eng.* 11:279–294.
9. Ionita, M. A., R. M. Ion, and B. Carstocea. 2003. Photochemical and photodynamic properties of vitamin B2-riboflavin and liposomes. *Oftalmologia.* 58:29–34.
10. Conlan, M. J., J. W. Rapley, and C. M. Cobb. 1996. Biostimulation of wound healing by low-energy laser irradiation. A review. *J. Clin. Periodontol.* 23:492–496.
11. Walsh, L. J. 1997. The current status of low level laser therapy in dentistry. Part 1. Soft tissue applications. *Aust. Dent. J.* 42:247–254.
12. Boulnois, J. L., and A. Morfino. 1983. *Minerva Med.* 74:1669–1673 [Photo-biomolecular effects of laser radiation].
13. Doukas, A. G., D. J. McAuliffe, and T. J. Flotte. 1993. Biological effects of laser-induced shock waves: structural and functional cell damage in vitro. *Ultrasound Med. Biol.* 19:137–146.
14. Doukas, A. G., D. J. McAuliffe, S. Lee, V. Venugopalan, and T. J. Flotte. 1995. Physical factors involved in stress-wave-induced cell injury: the effect of stress gradient. *Ultrasound Med. Biol.* 21:961–967.
15. Doukas, A. G., and T. J. Flotte. 1996. Physical characteristics and biological effects of laser-induced stress waves. *Ultrasound Med. Biol.* 22:151–164.
16. Thomsen, S. 1991. Pathologic analysis of photothermal and photomechanical effects of laser-tissue interactions. *Photochem. Photobiol.* 53:825–835.
17. Jansen, E. 2004. Laser tissue interactions, 1st ed. Encyclopedia of Biomaterials and Biomedical Engineering. Marcel Dekker, New York. 883–891.
18. Welch, A. J., and M. van Gemert. 1995. Optical-thermal response of laser irradiated tissue. Plenum Press, New York.
19. Telenkov, S. A., D. P. Dave, S. Setheruraman, T. Akkin, and T. E. Milner. 2004. Differential phase optical coherence probe for depth-resolved detection of photothermal response in tissue. *Phys. Med. Biol.* 49:111–119.
20. Rylander, C. G., D. P. Davé, T. Akkin, T. E. Milner, K. R. Diller, and A. J. Welch. 2004. Quantitative phase-contrast imaging of cells with phase-sensitive optical coherence microscopy. *Opt. Lett.* 29:1509–1511.
21. Kim, J., D. T. Miller, E. Kim, S. Oh, J. Oh, T. E. Milner. 2005. Optical coherence tomography speckle reduction by a partially spatially coherent source. *J. Biomed. Opt.* 10:064034.
22. Torres, J. H., T. A. Springer, A. J. Welch, and J. A. Pearce. 1990. Limitations of a thermal camera in measuring surface temperature of laser-irradiated tissues. *Lasers Surg. Med.* 10:510–523.
23. Waldman, G. 1983. Introduction to Light: The Physics of Light, Vision, and Color. Prentice-Hall, Englewood Cliffs, NJ.
24. Niemz, M. H. 2004. Laser-Tissue Interactions, 3rd ed. Springer, Berlin. 308.
25. Wells, J. D., P. Konrad, C. Kao, E. D. Jansen, and A. Mahadevan-Jansen. 2007. Pulsed laser versus electrical energy for peripheral nerve stimulation. *J. Neurosci. Methods.* 30:326–337.
26. Glickman, R., M. Natarajan, B. Rockwell, M. Denton, S. Maswadi, N. Kumar, and F. Nieves-Roldan. 2005. Intracellular signaling mechanisms responsive to laser-induced photochemical and thermal stress. *Proc. Soc. Photo Opt. Instrum. Eng.* 5695:260–269.
27. Hirase, H., V. Nikolenko, J. H. Goldberg, and R. Yuste. 2002. Multiphoton stimulation of neurons. *J. Neurobiol.* 51:237–247.
28. Norton, S. J. 2003. Can ultrasound be used to stimulate nerve tissue? *Biomed. Eng. Online.* 2:6.
29. Shusterman, V., P. J. Jannetta, B. Aysin, A. Beigel, M. Glukhovskoy, and I. Usiene. 2002. Direct mechanical stimulation of brainstem modulates cardiac rhythm and repolarization in humans. *J. Electrocardiol.* 35(Suppl):247–256.

30. Welch, A. J., and M. J. C. van Gemert. 1995. Optical-Thermal Response of Laser-Irradiated Tissue. Lasers, Photonics, and Electro-optics. Plenum Press, New York. xxvi, 925.

31. Jansen, E. D., M. Frenz, K. A. Kadipasaoglu, T. J. Pfefer, H. J. Altermatt, M. Motamedi, and A. J. Welch. 1997. Laser-tissue interaction during transmyocardial laser revascularization. *Ann. Thorac. Surg.* 63:640–647.

32. Incropera, F. P. 2002. Fundamentals of Heat and Mass Transfer, 5th ed. John Wiley and Sons, Hoboken, NJ.

33. van Gemert, M. J., and A. J. Welch. 1989. Time constants in thermal laser medicine. *Lasers Surg. Med.* 9:405–421.

34. Verdaasdonk, R. M., and C. Borst. 1991. Ray tracing of optically modified fiber tips. *Appl. Opt.* 30:2159–2171.

35. Borrelli, M. J., C. M. Rausch, R. Seaner, and G. Iliakis. 1991. Sensitization to hyperthermia by 3,3′-dipentyloxacarbocyanine iodide: a positive correlation with DNA damage and negative correlations with altered cell morphology, oxygen consumption inhibition, and reduced ATP levels. *Int. J. Hyperthermia.* 7:243–261.

36. Cole, A., and E. P. Armour. 1988. Ultrastructural study of mitochondrial damage in CHO cells exposed to hyperthermia. *Radiat. Res.* 115:421–435.

37. Izzo, A. D., C. P. Richter, E. D. Jansen, and J. D. Welch. 2006. Laser stimulation of the auditory nerve. *Lasers Surg. Med.* 38:745–753.

38. Jacques, S. L., and S. A. Prahl. 1987. Modeling optical and thermal distributions in tissue during laser irradiation. *Lasers Surg. Med.* 6:494–503.

39. Jacques, S. L., C. A. Alter, and S. A. Prahl. 1987. Angular dependence of HeNe laser light scattering by human dermis. *Lasers Life Science.* 1:309–334.

40. Kandel, E. R., J. H. Schwartz, and T. M. Jessell. 2000. Principles of Neural Science, 4th ed. McGraw-Hill, New York. xli, 1414.

41. Weiss, T. F. 1996. Cellular Biophysics. MIT Press, Cambridge, MA.

42. Frankenhaeuser, B., and L. E. Moore. 1963. The effect of temperature on the sodium and potassium permeability changes in myelinated nerve fibres of Xenopus laevis. *J. Physiol.* 169:431–437.

43. Moore, L. E. 1975. Membrane conductance changes in single nodes of Ranvier, measured by laser-induced temperature-jump experiments. *Biochim. Biophys. Acta.* 375:115–123.

44. Cesare, P., A. Moriondo, V. Vellani, and P. A. McNaughton. 1999. Ion channels gated by heat. *Proc. Natl. Acad. Sci. USA.* 96:7658–7663.

45. Tominaga, M., M. J. Caterina, A. B. Malmberg, T. A. Rosen, H. Gilbert, K. Skinner, B. E. Raumann, A. I. Basbaum, and D. Julius. 1998. The cloned capsaicin receptor integrates multiple pain-producing stimuli. *Neuron.* 21:531–543.

46. Nagy, I., and H. Rang. 1999. Noxious heat activates all capsaicin-sensitive and also a sub-population of capsaicin-insensitive dorsal root ganglion neurons. *Neuroscience.* 88:995–997.

47. Cesare, P., and P. McNaughton. 1996. A novel heat-activated current in nociceptive neurons and its sensitization by bradykinin. *Proc. Natl. Acad. Sci. USA.* 93:15435–15439.

48. Benham, C. D., M. J. Gunthorpe, and J. B. Davis. 2003. TRPV channels as temperature sensors. *Cell Calcium.* 33:479–487.

49. Liman, E. R. 2006. Thermal gating of TRP ion channels: food for thought? *Sci. STKE.* 2006:pe12.

50. Liu, B., K. Hui, and F. Qin. 2003. Thermodynamics of heat activation of single capsaicin ion channels VR1. *Biophys. J.* 85:2988–3006.